Engineering Conferences International
ECI Digital Archives

10th International Conference on Circulating Fluidized Beds and Fluidization Technology - CFB-10

Refereed Proceedings

Spring 5-2-2011

Cold Model Investigations of a High Temperature Looping Process in a Dual Circulating Fluidized Bed System

Ajay R. Bidwe
Institute of Combustion and Power Plan Technology, University of Stuttgart

Miguel A.M Dominguez
Institute of Combustion and Power Plan Technology, University of Stuttgart

Craig Hawthorne
Institute of Combustion and Power Plan Technology, University of Stuttgart

Heiko Dieter
Institute of Combustion and Power Plan Technology, University of Stuttgart

Alexander Charitos
Institute of Combustion and Power Plan Technology, University of Stuttgart

See next page for additional authors

Follow this and additional works at: http://dc.engconfintl.org/cfb10

 Part of the Chemical Engineering Commons

Recommended Citation

Ajay R. Bidwe, Miguel A.M Dominguez, Craig Hawthorne, Heiko Dieter, Alexander Charitos, Anjia Schuster, and Güenter Scheffknecht, "Cold Model Investigations of a High Temperature Looping Process in a Dual Circulating Fluidized Bed System" in "10th International Conference on Circulating Fluidized Beds and Fluidization Technology - CFB-10", T. Knowlton, PSRI Eds, ECI Symposium Series, (2013). http://dc.engconfintl.org/cfb10/8

This Conference Proceeding is brought to you for free and open access by the Refereed Proceedings at ECI Digital Archives. It has been accepted for inclusion in 10th International Conference on Circulating Fluidized Beds and Fluidization Technology - CFB-10 by an authorized administrator of ECI Digital Archives. For more information, please contact franco@bepress.com.

Authors
Ajay R. Bidwe, Miguel A.M Dominguez, Craig Hawthorne, Heiko Dieter, Alexander Charitos, Anjia Schuster, and Güenter Scheffknecht

This conference proceeding is available at ECI Digital Archives: http://dc.engconfintl.org/cfb10/8

COLD MODEL INVESTIGATIONS OF A HIGH TEMPERATURE LOOPING PROCESS IN A DUAL CIRCULATING FLUIDIZED BED SYSTEM

Ajay R. Bidwe, Miguel A.M. Dominguez, Craig Hawthorne, Heiko Dieter, Alexander Charitos, Anja Schuster, Günter Scheffknecht

Institute of Combustion and Power plant technology (IFK), University of Stuttgart, Pfaffenwaldring 23, 70569, Stuttgart, Germany.
Email: bidwe@ifk.uni-stuttgart.de

ABSTRACT

The Calcium Looping process is a promising post-combustion CO_2 capture technology. A 200 kW_{th} Dual Circulating Fluidized Bed has been built at IFK, University of Stuttgart. Tests were carried out on a hydrodynamically scaled cold model. Operating parameters have been varied, while the suitability of the 200 kW_{th} design has been proven.

INTRODUCTION

It is now evident that the anthropogenic CO_2 emissions are causing serious global warming. Coal and natural gas based power plants are the major source of CO_2 emissions and cause nearly 30 % of global CO_2 emissions (1). Various pre- and post-combustion CO_2 capture options are currently under investigation. One of the attractive options is the Calcium Looping (CaL) process which can be integrated with the existing power plants (2). The CaL process has the advantage of low efficiency penalties of 4 to 6% (3) and can be economical compared to other suggested methods (3). The basic reaction of the Calcium Looping Process is given in Eq. 1.

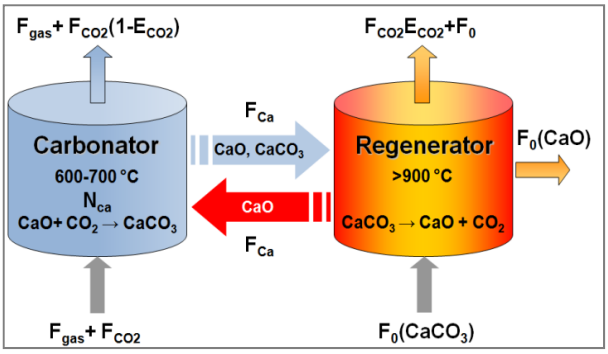

Figure 1- Scheme of Calcium Looping process

$$CaO_{(s)} + CO_{2\,(g)} \leftrightarrow CaCO_{3(s)} \quad (1)$$

A schematic of the CaL process is shown in Fig. 1. This process was first suggested by Shimizu et al. (4). It consists of the carbonator and the regenerator for the CO_2 capture and the sorbent regeneration, respectively. The CO_2 rich flue gases are fed into carbonator where CO_2 reacts with CaO to form $CaCO_3$ at 600-700°C. As a result a CO_2 lean gas can is released from the carbonator. The formed $CaCO_3$ is transferred to the regenerator where at >900 °C CO_2 is released again. The sorbent (CaO) is regenerated by the reverse reaction of Eq. 1. Since the regeneration step requires energy to heat up and support the endothermic reaction at 900°C; an

oxyfuel combustion is conducted in the regenerator. The exit stream of the regenerator is CO_2 rich, and after compression can be stored geologically (2). The most suitable reactors are the dual fluidized bed reactors (DFB) and the process has been successfully demonstrated in various DFB facilities (5)(6). Blamey et al. (2) reviewed the CaL process as matured enough for a stage of pilot scale demonstration.

200 kW_{th} Pilot Plant at IFK, University of Stuttgart

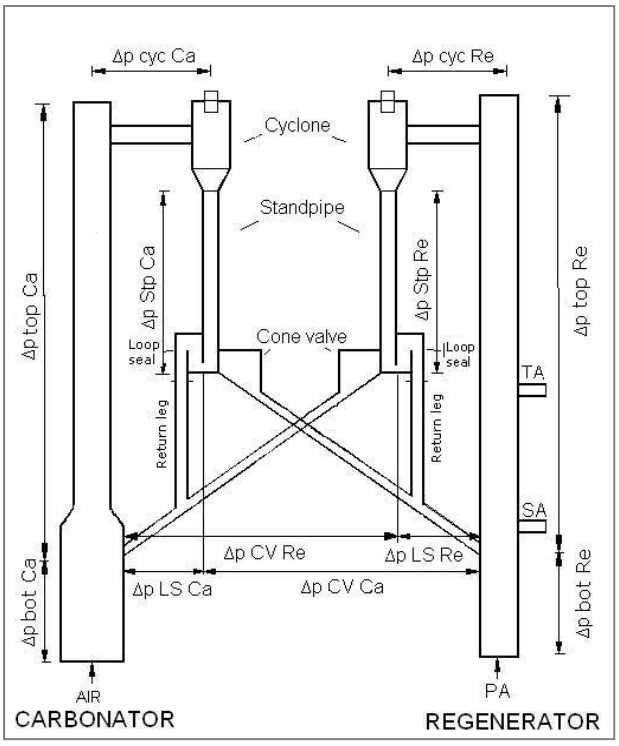

Figure 2 - Schematic of DCFB pilot plant and cold model for CO_2 capture using CaO as sorbent and important pressure drops considered in pressure balance

At IFK, University of Stuttgart, to realize the application of CaL process at pilot scale a dual circulating fluidized bed (DCFB) with a capacity of 200 kW_{th} has been installed (7). The schematic is shown in Fig. 2, where the carbonator and the regenerator are circulating fluidized beds (CFB) and are connected together by cone valves for the solid looping between the reactors. In previous studies at IFK, CFB reactors as carbonator were found to be kinetically more effective than the bubbling fluidized bed (BFB) (5)(6). In the regenerator the heat is generated by the combustion of fuels. A CFB is commercially well proven for its ability as a combustor (8). Therefore the regenerator is also selected as a CFB. The Cone valve is a mechanical valve which is used also in commercial CFB boilers for transporting material to the external heat exchangers (9). Charitos et al. (5) used the cone valve to control the solid looping rate between two fluidized beds effectively. The cone valve offers the control and variation of the looping rate independent of the fluidization velocities in the reactors and thus allows a high flexibility in operation.

The twin cone valve coupled DCFB system at IFK is a new process concept. In order to support the design of the pilot plant, a scaled cold flow model has been built and operated under conditions scaled to the real conditions in the pilot plant. The aim of this paper is summarized as follows a) Prove the hydrodynamic feasibility of this novel DCFB concept shown in Fig. 2 b) Testing of the cold model and operational boundary conditions. c) Investigate the effect of important operational parameters on the operation of the DCFB and find out the optimum way to control the solid looping rates. The operational parameters are stated in Table 1. The test will show if the required riser inventories, entrainment rates and solid looping rates can be met in the pilot plant.

DCFB Cold Model Description

As shown in Fig. 2 the pilot plant consists of two CFBs namely the carbonator and the regenerator. Table 1 shows the important dimensions of the carbonator and the regenerator. A detailed description of the 200 kW_{th} pilot plant can be found in (7). Each CFB has its own internal circulating system comprising of *riser - cyclone – standpipe – loop seal - return leg - riser*. Both CFBs reactors are connected by the cone valves which are placed at the bottom of the loop seals on the supply side of the standpipes. The discharge of each cone valve is directed to the other reactor.

The cold model, shown in Fig. 2 is geometrically scaled in the ratio of 1:2.5. This ratio is also maintained for other components of the fluidized bed, i.e. standpipes, loop seals, etc. The cold model presented in this study is based on the scaling laws developed by Glicksmann (10). The complete set of equations is given in Eq. 2.

$$\frac{u_o^2}{gL}, \frac{\rho_s}{\rho_g}, \frac{u_o}{u_{mf}}, \frac{L_1}{L_2}, \frac{G_s}{\rho_s u_o}, \frac{\Delta p_{riser}}{\rho_s g D_{riser}}, \phi, PSD \qquad (2)$$

Basic operational values of the cold model derived from the application of the above mentioned scaling laws are listed in Table 1. The particles were chosen in order to match the density ratio of Eq. 1 for the carbonator. The required particle density for these experiments is 5440 kg/m³. Iron oxide (Fe_3O_4) particles with a particle density of 5170 kg/m³ have been chosen. The particle size distribution (PSD) was 100 to 200 µm with a mean size of 166 µm. This PSD at cold flow scale corresponds to a PSD of about 300-500 µm for the conditions in the pilot plant. Moreover, the gas density in the regenerator is different than in the carbonator due to different gas composition and higher temperatures. The gas density of the regenerator is thus adjusted by using a mixture of CO_2 and air, whereas the carbonator is operated on air. The operational parameters considered in this study are the riser velocity, the total solid inventory and cone valve opening. While parameters such as riser pressure drop (Δp_{riser}), riser inventory (W_{riser}), entrainment rate (G_s) and cone valve flow rate (G_{cv}) are obtained as experimental results. The experimental results from the cold model are extrapolated to the pilot plant scale using the ratios shown in Table 1. These ratios are derived from Eq. 2. For example the pressure term in Eq. 2 for the hot pilot and cold model can be matched and $\frac{\Delta p_{riser\ pilot}}{\Delta p_{riser\ cold}} = 0.87$ is obtained from geometric ratio and particle densities of the hot plant and cold model.

Experimental Procedure

Since the regeneration of the sorbent will be conducted with high O_2/CO_2 ratios in the real process, oxidant staging is necessary in order to avoid temperature hot spots in the hot facility. Moreover oxidant staging will improve the combustion quality. Therefore, the pilot plant regenerator will have different axial velocity profiles. For the cold model experiments, a combined velocity rise due to air staging and gas release is simulated and the scaled velocity is applied with three air stages. The air in both risers is supplied by a blower and the gas flow rates are measured by the rotameters. Pressure drop measurements are recorded in different positions at the cold model using pressure transducers and a data acquisition system. During the experiment the following parameters are varied: carbonator velocity ($u_{0\ Ca}$), regenerator velocity ($u_{0\ Re}$), regenerator air staging ratio, total solid inventory (TSI) and cone valve openings ($A_{cv\ Ca}$, $A_{cv\ Re}$). Both riser circulation rates are determined

by stopping the loop seal aeration and measuring the time required to achieve a specific increase of the solid level in the standpipe. Cone valve flow rates are measured by diverting the cone valve flow into sampling ports, situated below the cone valves. Flow diversion is done for a specific time and the sample is subsequently weighed.

Table 1 – Basic values of cold model and 200 kW_{th} Calcium looping DCFB pilot plant

Parameter	Unit	Carbonator		Regenerator		Ratio
		Pilot plant	Cold model	Pilot plant	Cold model	$\frac{Pilot\ plant}{cold\ model}$
D_{riser}	m	0.23	0.092	0.17	0.069	2.5
L_{riser}	m	10	4	10	4	2.5
T	°C	650-700	20	850-900	20	
ρ_s	kg/m³	1800	5170	1800	5170	
ρ_g	kg/m³	0.39	1.18	0.44	1.26	
u_0	m/s	4-6	2.5-4	4-6	2.5-4	1.58
Δp_{riser}	mbar	100	115	60-80	69-92	0.87
G_s	kg/m²s	5-25	10-45	10-40	15-70	0.55
G_{cv}	kg/h	500-1200		500-1200		
W_{riser}	kg	30-50	5.52-9.05			5.43

Pressure Balance

As seen in Fig. 2 there are two clear distinct pressure balance loops for each CFB, i.e. *riser-cyclone-standpipe-loop seal-riser-loop-return leg*. The pressure balance for this loop can be described as follows in Eq. 3 and Eq. 4. This is similar to what has found in other works on CFB loop (11)(12).

$$\Delta p_{stp\ Ca} = \Delta p_{LS\ Ca} + \Delta p_{top\ CA} + \Delta p_{cyc\ Ca} \quad (3)$$

$$\Delta p_{stp\ Re} = \Delta p_{LS\ Re} + \Delta p_{top\ Re} + \Delta p_{cyc\ Re} \quad (4)$$

$\Delta p_{top\ Ca}$ and $\Delta p_{top\ Re}$ are the pressure drops in the riser above the return leg of the loop seal. The pressure drop between the distributor and the return leg entrance ($\Delta p_{bot\ Ca}$ and $\Delta p_{bot\ Re}$) does not take part in the pressure balance. The total pressure drop in the riser is the sum of $\Delta p_{bot\ i}$ and $\Delta p_{top\ i}$.

However, in the present DCFB system, there exists another loop linking carbonator and regenerator similar to Eq. 3 and Eq. 4. The pressure balance for this loop can be described as follows in Eq. 5 and Eq. 6.

$$p_{Re\ exit} + \Delta p_{stpRe} = \Delta p_{CVRe} + \Delta p_{top\ Ca} + \Delta p_{cycCa} + p_{Ca\ exit} \quad (5)$$

$$p_{Ca\ exit} + \Delta p_{stpCa} = \Delta p_{CVCa} + \Delta p_{top\ Re} + \Delta p_{cycRe} + p_{Re\ exit} \quad (6)$$

The absolute pressure at the exit $p_{i\ exit}$ and standpipe pressure drop Δp_{stpi} of one CFB equals the sum of the cone valve pressure drop Δp_{CVi}, riser top $\Delta p_{top\ i}$, cyclone pressure drop $\Delta p_{cyc\ i}$ and absolute exit pressure of the other CFB $p_{i\ exit}$. Eq. 7 is the cone valve characteristic equation deduced from Charitos et al. (12). It shows the relation between flow rate and pressure drop across the valve and its opening.

$$G_{CV} = k\ A_{CV} \Delta p_{CV} \quad (7)$$

In order to ensure mass flow through the cone valve, the pressure at the bottom of the standpipe should be sufficiently high to overcome the pressure in the other

reactor. It is very important that both cone valves deliver equal amounts of mass in order to provide a hydrodynamic steady state for the entire solid looping process.

RESULTS AND DISCUSSION

Hydrodynamics of Single Loop Carbonator

Fig. 3 shows the effect of the superficial velocity on the riser inventory. During the tests only the carbonator has been operated and the total solid inventory (TSI) kept constant. The total riser inventory clearly decreases with increasing superficial velocity. This fact is a result of the pressure balance, since a raise in velocity increases the mass in the riser top region of the riser as shown in Fig. 3 and thus taking part in the pressure balance. To balance this increased pressure drop $\Delta p_{Ca\ top}$ the standpipe should create enough Δp_{stpCa} according to Eq. 2. This is accomplished by adjusting the required mass from the riser bottom to the standpipe. The decrease of inventory in the riser bottom is a proof of this.

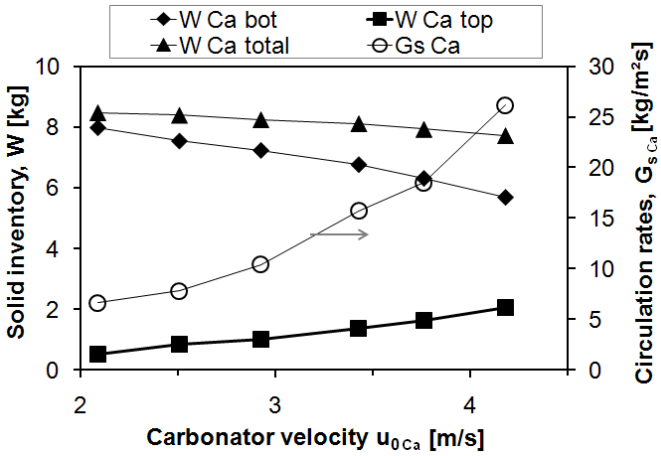

Figure 3 - Effect of carbonator velocity on inventory and circulation rates.

The inventory carried by the riser is determined to 8.5 kg at 2 m/s which corresponds to 46.1 kg for the pilot plant extrapolated by scaling ratios (see Table 1). This amount is within the inventory range required in the pilot plant. Moreover Fig. 3 shows an increase of circulation rate Gs (measured after the cyclone). This results from the velocity increase in the carbonator and shows that the circulation rates are directly related to the velocity. The circulation rate varies from 6.6 to 26.1 kg/m²s and corresponds to 3.64 to 14.38 kg/m²s or 545 to 2150 kg/h extrapolated to the pilot plant using scaling ratios in Table 1. Furthermore, the circulation rate (G_s) should be higher than cone valve (G_{cv}) flow rate. The cone valve flow rates required in the pilot plant are in the range of 500 to 1200 kg/h, thus circulation rates projections from carbonator are satisfactory.

Coupled DCFB Behaviour

The most important aspect of the cold model investigations was to prove the feasibility of a DCFB system interconnected with two cone valves. The pressure balance as explained earlier shows that reactors, connected with two cone valves are hydrodynamically linked. Therefore, single parameters affecting the pressure balance will influence the hydrodynamics of both reactors. For the operation of a coupled DCFB system, the effect of parameter variations, such as riser velocities, solid inventory, cone valve openings and its effect on the cone valve flow rate as well as riser hydrodynamics were studied. For a given set of riser velocities, the total solid inventory, the cone valve opening, the cone valve flow rate and the riser pressure drops were always adjusted according to the pressure balance

established. The mass flow rates at both cone valves were equal. Variations of the riser velocity or the solid inventory have effect on the cone valve mass flow rates. The inventory transfer between both reactors achieves a stable point with a stable pressure balance and flow conditions. This behaviour can be seen in Fig. 6 and 7. The most reliable way to control the flow rates is to change the opening of the cone valves. In the experiments of Fig. 4 the u_0 in both risers and TSI in the system was kept constant and only A_{cv} in both CFB was varied. With increasing cone valve opening the flow rate increased. The cone valves used in this study were geometrically identical and flow rates measured had little deviation as observed in Fig. 4.

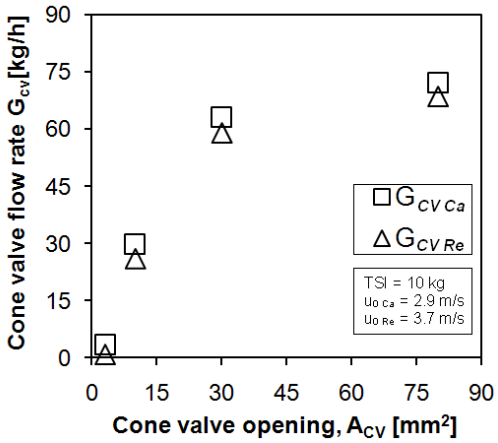

Figure 4 - Variation of cone valve flow with opening

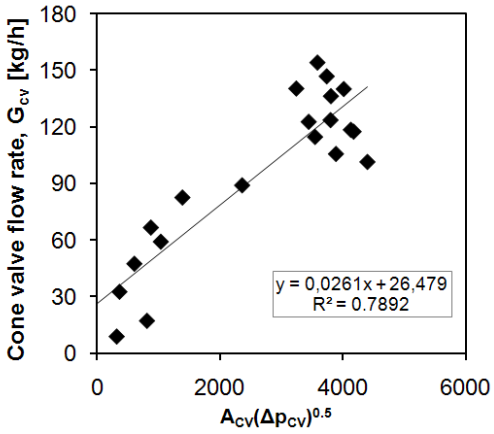

Figure 5 - Cone valve characteristics

Cone Valve Characterization

In Fig. 5 the variation of cone valve flow rate G_{cv} is shown with the product of area of the cone valve and square root of the pressure drop across the valve. A linear curve with a satisfactory fit could be observed. The final equation of the cone valve mass flow is given in Eq. 8. The deduced empirical Eq. 8 is according to equations found in the literature (13), where the solid flow through mechanical valves is a function of the opening area and square root of the pressure drop across the valve.

$$G_{CV} = 0.0261 A_{CV} \Delta p_{CV}^{0.5} + 26.479 \qquad (8)$$

Regenerator Hydrodynamics at Different Air Staging Ratios

In Fig. 6 and Fig. 7 the effect of air staging in the regenerator on the operational conditions in the coupled DCFB system is presented. During these experiments, the conditions in the carbonator, the total solid inventory (TSI) and the cone valve openings (A_{cv}) were kept constant. The total volumetric flow rate (VFR) in the regenerator was kept constant at 50 m³/h therefore final $u_{0\,Re}$ is equal to 3.7 m/s. The required VFR in the regenerator is divided into primary air (PA), secondary air (SA) and tertiary air (TA) as shown in Fig. 2. Fig. 6 shows that with increasing PA, the regenerator pressure drop Δp_{Re} decreases from 73 to 34 mbar and at the same time the carbonator pressure drop Δp_{Ca} increases from 61 to 70 mbar giving an indication that the bed inventory is transferred from the regenerator to the carbonator. The raise in the carbonator pressure drop Δp_{Ca} is lower compared to the regenerator

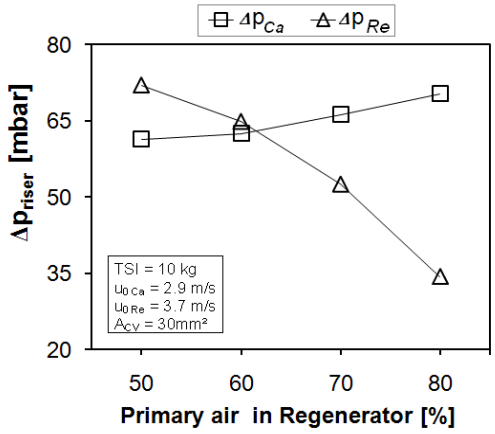

Figure 6 - Effect of air staging in regenerator on inventory distribution in DCFB system

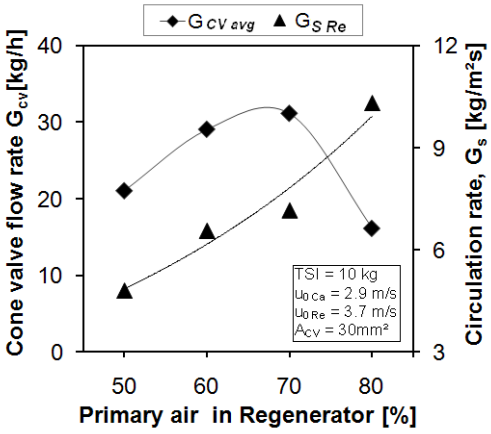

Figure 7 - Effect of air staging on circulation rates and cone valve flow (Regenerator)

pressure drop Δp_{Re} because of the larger diameter of the carbonator. From the present results it becomes obvious that the pressure balances in the coupled DCFB system play an important role. More primary air shifts more mass towards the upper region of regenerator. This increases the regenerator standpipe pressure Δp_{stpRe} according to Eq. 4 and Eq. 5 Δp_{Ca} increases. An increase of primary air has a major effect on the solid flow rate in the regenerator Gs_{Re} as seen in Fig. 7 and is the main driving force for the change of circulation rate in the regenerator. The amount of primary air can also increase the cone valve flow rate G_{CV} rates as given in Eq. 6, but due to transfer of inventory and changes of pressure values this increase is limited.

CONCLUSIONS

The scaled cold model investigations of the proposed DCFB system at IFK, University Stuttgart have been performed. The coupling of two CFB reactors, interconnected with two cone valves is possible. The flow rate between the beds can be controlled by the two cone valves and has a characteristic equation. The pressure balance plays an important role for the inventory distribution and cone valve flow rate. The cold model was investigated within the required design range, corresponding to the planned pilot plant. By means of this investigation, the design of the planned 200 kW_{th} pilot plant was approved.

ACKNOWLEDGEMENTS

We thank EnBW Kraftwerke AG for the funding of this research project.

NOTATION

A_{cv}	mm^2	area of cone valve	T	°C	temperature
D	m	diameter	$u_{0\,i}$	m/s	superficial velocity of riser i
g	m/s^2	gravitational acceleration	u_{mf}	m/s	minimum fluidization velocity
G_{CV}	kg/h	cone valve flow rate	W	kg	solid inventory
G_s	kg/m^2s	riser circulation rate	Δp_i	mbar	pressure drop in *i*

L	m	dimension of a component	ρ_g	kg/m³	gas density
$\emptyset$	[-]	sphericity of particles	ρ_s	kg/m³	particle density

Abbreviations

CFB	Circulating fluidized bed	PSD	Particle size distribution
CV	Cone valve	SA	Secondary air
DCFB	Dual circulating fluidized bed	Stp	Standpipe
DFB	Dual fluidized bed	TA	Tertiary air
LS	Loop seal	TSI	Total solid inventory
PA	Primary air	VFR	Volumetric flow rate

Subscripts component i

Ca	carbonator
Re	regenerator
top	Part of riser above return leg from loop seal till exit.
bot	Part of riser between distributor and loop seal return leg inlet.

REFERENCES

1. Mondol J.B., McIlveen-Wrighta D., Rezvania S., Ye Huanga and Hewitt N., (2009), “Techno-economic evaluation of advanced IGCC lignite coal fuelled power plantsnext term with CO_2 capture”, *Fuel,* 88 (12), 2495-2506.
2. Blamey J., Anthony E.J., Wang J., Fennell P.S., (2010), "The calcium looping cycle for large-scale CO_2 capture", *Progress in Energy and Combustion Science,* 36 (2), 260-279.
3. Hawthorne C., Trossmann M., Galindo Cifre P., Schuster A. and Scheffknecht G. (2009), "Simulation of the carbonate looping power cycle", *Energy Procedia,* 1, 1387-1394.
4. Shimizu T., Hirama T., Hosoda H. and Kitano K. A., (1999), ’’Twin fluid-bed reactor for removal of CO_2 from combustion processes", *Chemical Engineering Research and Design*, 77 (1), 62- 68.
5. Charitos A., Hawthorne C., Bidwe A.R., Sivalingam S., Schuster A., Spliethoff H. and Scheffknecht G., (2010), "Parametric investigation of the calcium looping process for CO_2 capture in a 10 kW_{th} dual fluidized bed.", *Int. J. of greenhouse gas control*, 4 (5), 776-784.
6. Rodriguez N., Alonso M., Abanades J.C., Charitos C., Hawthorne C., Scheffknecht G., Lu D.Y. and Anthony E.J., (2010), “Comparison of experimental results from three dual fluidized bed test facilities capturing CO_2 with CaO”, *In proceeding: GHGT-10 Amsterdam* (19-23 Sep 2010).
7. Hawthorne C., Dieter H., Bidwe A., Schuster A., Scheffknecht G., Unterberger S. and Käß M., (2010), “CO_2 capture with CaO in a 200 kW_{th} dual fluidized bed pilot plant”, *In proceeding: GHGT-10 Amsterdam* (19-23 Sep 2010).
8. Basu P., (2006), "Combustion and Gasification in Fluidized Beds”. Taylor & Francis Group.
9. Wang Q., Luo Z., Fang M., Ni M. and Cen K., (2003), "Development of a new external heat exchanger for a circulating fluidized bed boiler", *Chemical Engineering and Processing,* 42 (4), 327-335.
10. Glicksman L.R., (1993), "Simplified scaling relationships for fluidized bed'.', *Powder Technology*, 77 (2), 177-199.
11. Basu P. and Cheng L.,(2000), "An analysis of loop seal operations in a circulating fluidized bed”. *Chemical Engineering Research and Design*, 78 (7), 991-998.
12. Charitos A. Hawthorne C., Bidwe A.R., Korovesis L., Schuster A. and Scheffknecht G. (2010), "Hydrodynamic analysis of a 10 kW_{th} calcium looping dual fluidized bed for post-combustion CO_2 capture", *Powder Technology*, 200 (3), 117–127.
13. Davidson. J.F and Jones D.R.M. (1965), "The flow of particles from a fludized bed through an orifice", *Rheologica Acta* 4, 180-192.